CellPress

What's the Key to Unlocking the Proteasome's Gate?

Andres H. de la Peña[1] and Gabriel C. Lander[1,*]
[1]Department of Integrative Structural and Computational Biology, The Scripps Research Institute, 10550 N. Torrey Pines Rd, La Jolla, CA 92037, USA
*Correspondence: glander@scripps.edu
http://dx.doi.org/10.1016/j.str.2016.11.011

In this issue of *Structure*, Bolten et al. (2016) describe the organization of the mycobacterial proteasome in complex with the ATP-independent bacterial proteasome activator (Bpa, PafE). They confirm several activation motifs employed by archaea and eukaryotes and highlight differences that pose Bpa as a novel architectural class of proteasome activators.

As the primary effector of targeted protein degradation, the proteasome is central to many physiological processes, from mitosis to antigen presentation. To safeguard against indiscriminate protein degradation, access to the proteasomal catalytic chamber is tightly regulated through a gating mechanism that requires the attachment of an activator protein complex. The pivotal role that these activators play in protein degradation has been the focus of many biochemical, biophysical, and structural studies, yet the precise mechanism by which these protein complexes trigger proteasome core (20S) gate opening remains to be elucidated.

These proteasome activator complexes, which assemble through elaborate pathways, have flexible termini, a high molecular mass, and exhibit micromolar binding affinities for the 20S, have eluded crystallization and high-resolution structure determination for many years. Recently, the advent of direct detectors in cryo-electron microscopy (cryo-EM) has enabled detailed structural analyses of the 20S in complex with ATP-independent (Bai et al., 2016; Bolten et al., 2016) and ATP-dependent (Chen et al., 2016; Huang et al., 2016; Schweitzer et al., 2016) activators. These studies confirmed previous reports that activators attach to the 20S via a C-terminal motif. However, these studies also revealed that the proteasome gate differs significantly across species and that activators may employ unique gate opening mechanisms. Furthermore, these studies evidence a general trend of heightened interest in these large macromolecular structures, which will continue to increase as cryo-EM becomes more widely accessible (Figure 1).

The proteasome core (20S) is composed of four heptameric rings of α- and β-subunits stacked in a barrel-like $\alpha_7\beta_7\beta_7\alpha_7$ arrangement (Figure 2A). The β-rings catalyze substrate hydrolysis, whereas the α-subunits are involved in gating and activator binding. The 20S architecture is highly conserved from bacteria to eukarya, whereas activators exhibit diversity and varying degrees of complexity, from monomeric Blm10 to the 19-subunit regulatory particle (19S) (Figure 2B). In this issue of *Structure*, Bolten et al. (2016) present the cryo-EM structure of the *Mycobacterium tuberculosis* bacterial proteasome activator Bpa in complex with 20S at a nominal resolution of 3.5 Å, shedding new light on activator: proteasome interactions. Importantly, their structure reveals the existence of a salt bridge between the Bpa C-terminal α-carboxylate and the 20S binding pocket, confirming that the α-carboxylate motif, first observed in archaea and eukarya, is present across all domains of life.

Bolten et al. (2016) utilized a combination of X-ray crystallography and single particle cryo-EM to examine the atomic-level details of Bpa's interactions with *M. tuberculosis* 20S. Crystal structures of Bpa are consistent with the recent structural findings from Bai et al. (2016) showing that the Bpa protomer comprises an antiparallel four-helix bundle similar to the α-helical folds observed in 11S protomers. However, unlike all other activators known to date, Bpa forms an active dodecameric ring assembly with a striking symmetry mismatch at the heptameric 20S interface. This mismatch likely results in partial occupancy of the seven available "docking pockets" at the 20S interface. Bpa differs from other ATP-independent activators in that it possesses a larger pore (40 Å wide) and an extended 21-residue C-terminal

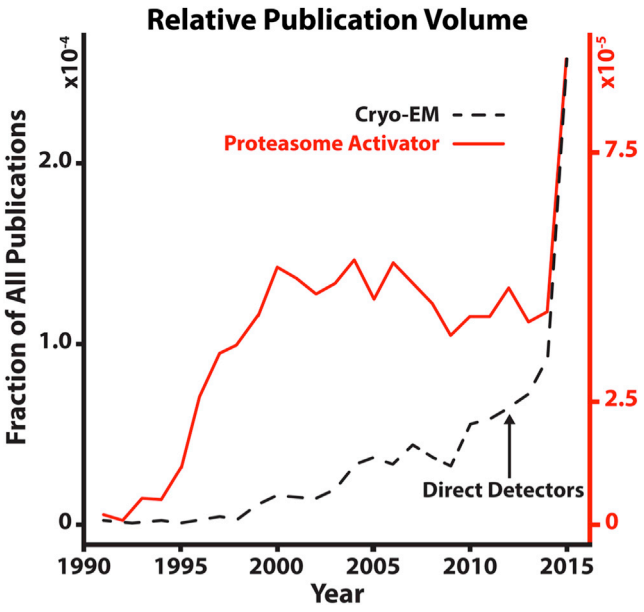

Figure 1. Relative Publication Volume
"Cryo-EM" and "Proteasome Activator*" search term results as a fraction of all cited works in the Web of Science Core Collection. Data analysis performed with the NAILS software (Knutas et al., 2015). The implementation of direct electron detectors for single particle cryo-EM is indicated by a black arrow.

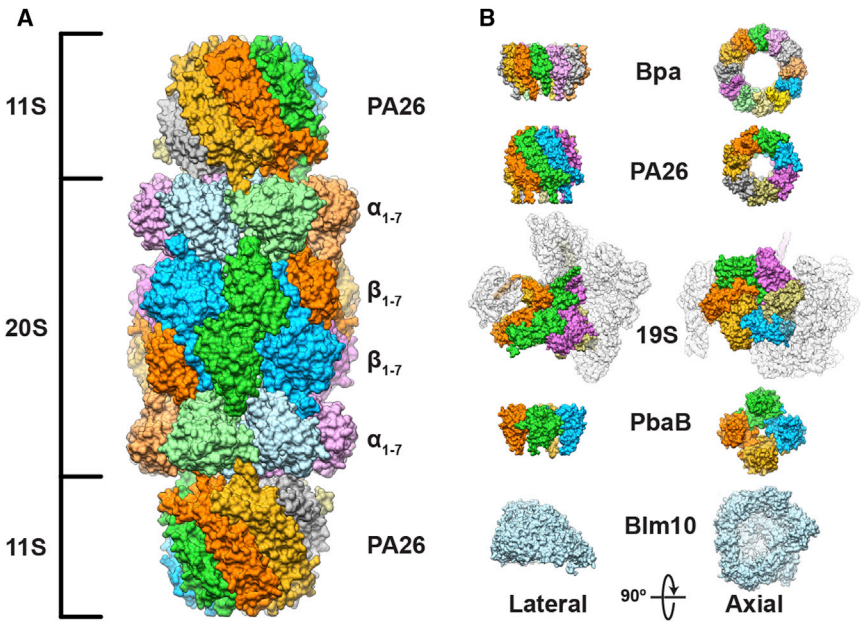

Figure 2. Architectural Classes that Bind the Proteasome
(A) Subunit composition of the *S. cerevisiae* 20S peptidase in complex with the *T. brucei* 11S activator (PA26).
(B) Proteasome activators from *M. tuberculosis* (Bpa dodecamer), *T. brucei* (11S heptamer), *H. sapiens* (19S hexameric AAA-ATPase with additional subunits), *P. furiosus* (PbaB tetramer), and *S. cerevisiae* (Bml10 monomer).

protrusion. These elongated termini give rise to a gap of ~20 Å between the Bpa and 20S pores. Bolten et al. (2016) note that this architecture resembles a "molecular funnel" and suggest that it performs a physiological function in recruiting substrates to the proteasome. This is in agreement with the observation by Bai et al. (2016) that the inner channel of the Bpa funnel is substantially hydrophobic compared to 11S activators, supporting the notion that Bpa can attract and thread small unfolded proteins into the proteasome.

To resolve the atomic interactions between Bpa and 20S, Bolten et al. (2016) employed DNA-encoded site-specific crosslinking to stabilize the Bpa:20S complex for single particle cryo-EM reconstruction. To maximize complex formation, a 20S mutant lacking the first seven residues of the α-subunit was utilized. The use of this mutant, which biases to 20S to adopt an "open gate" conformation, complements the structural study by Bai et al. (2016), where a Bpa C-terminal truncation was used to maximize complex formation. The resulting structure shows that the C-terminal α-carboxylate within the Bpa GQYL motif forms a salt bridge with a lysine at the base of the 20S docking pocket, a binding mechanism that is shared with all other activator:20S complexes determined to date. Similar interactions have also been observed in PA26 (Förster et al., 2005), PbaB (Kumoi et al., 2013), Blm10 (Sadre-Bazzaz et al., 2010), and 19S (Huang et al., 2016) proteasome complexes, in which a C-terminal HbYX motif analogous to GQYL is utilized for proteasome binding. The invariant "penultimate tyrosine" serves an analogous role in both motifs, establishing a cation-π stacking interaction with an arginine in the 20S docking pocket. However, Bolten et al. (2016) also observe distinguishing features between these motifs. The contrasting properties of the hydrophobic HbYX residue (Hb) and its GQYL counterpart (Q) extend beyond this motif, positioning the upstream residues in disparate conformations. Furthermore, the observed Mycobacterial 20S gate differs substantially from eukaryotic and archaeal gates (Stadtmueller and Hill, 2011), precluding comparisons to the putative activation mechanisms utilized by 11S and 19S activators. Overall, these results suggest a diverse array of mechanisms for gate opening, which partly explains why a consensus mechanism for gate opening has not emerged, despite numerous recent high-resolution cryo-EM reconstructions of activators bound to 20S.

Importantly, these structural discoveries have brought into question the long-standing models for proteasome activation, gate opening, and regulation. The Bpa structure suggests there may be additional mechanisms for both targeting proteins for degradation and regulating proteasome activity. The function of proteasome activators may be as diverse as their architectures, and understanding the atomic intricacies of their activation mechanisms will become vital as groups aim to develop targeted cancer and infectious disease therapies in the face of a highly conserved 20S.

REFERENCES

Bai, L., Hu, K., Wang, T., Jastrab, J.B., Darwin, K.H., and Li, H. (2016). Proc. Natl. Acad. Sci. USA *113*, E1983–E1992.

Bolten, M., Delley, C.L., Leibundgut, M., Boehringer, D., Ban, N., and Weber-Ban, E. (2016). Structure *24*, this issue, 2138–2151.

Chen, S., Wu, J., Lu, Y., Ma, Y.B., Lee, B.H., Yu, Z., Ouyang, Q., Finley, D.J., Kirschner, M.W., and Mao, Y. (2016). Proc. Natl. Acad. Sci. USA *113*, 12991–12996.

Förster, A., Masters, E.I., Whitby, F.G., Robinson, H., and Hill, C.P. (2005). Mol. Cell *18*, 589–599.

Huang, X., Luan, B., Wu, J., and Shi, Y. (2016). Nat. Struct. Mol. Biol. *23*, 778–785.

Knutas, A., Hajikhani, A., Salminen, J., Ikonen, J., and Porras, J. (2015). Cloud-based bibliometric analysis service for systematic mapping studies. B., Rachev and A. Smrikarov, eds. CompSysTech '15: Proceedings of the 16th International Conference on Computer Systems and Technologies, 184–191.

Kumoi, K., Satoh, T., Murata, K., Hiromoto, T., Mizushima, T., Kamiya, Y., Noda, M., Uchiyama, S., Yagi, H., and Kato, K. (2013). PLoS One *8*, e60294.

Sadre-Bazzaz, K., Whitby, F.G., Robinson, H., Formosa, T., and Hill, C.P. (2010). Mol. Cell *37*, 728–735.

Schweitzer, A., Aufderheide, A., Rudack, T., Beck, F., Pfeifer, G., Plitzko, J.M., Sakata, E., Schulten, K., Förster, F., and Baumeister, W. (2016). Proc. Natl. Acad. Sci. USA *113*, 7816–7821.

Stadtmueller, B.M., and Hill, C.P. (2011). Mol. Cell *41*, 8–19.